

Improved Direct Torque Control Load Torque Estimator with the Influence of Steering Angle for Dual Induction Motors Electric Vehicle Traction Drive System

¹Zulkifilie Ibrahim, ²Nurazlin Mohd Yaakop, ³Fauzi Ahmad,
¹Marizan Sulaiman, ⁴Kamaruzaman Jusoff, ⁵Zanariah Jano,
⁵Linda Khoo Mei Sui, ¹Ahmad Shukri Abu Hasim and ¹Siti Noormiza Mat Isa

¹Centre of Excellence for Robotics and Industrial Automation (CERIA),
Faculty of Electrical Engineering, Universiti Teknikal Malaysia Melaka (UteM),
Hang Tuah Jaya, 76100, Durian Tunggal, Melaka, Malaysia

²University Kuala Lumpur, Kulim Hi-Tech Park, 09000, Kulim, Kedah, Malaysia

³Centre of Vehicle Research and Development (CeVReD),
Faculty of Mechanical Engineering, Universiti Teknikal Malaysia Melaka (UteM),
Hang Tuah Jaya, 76100, Durian Tunggal, Melaka, Malaysia

⁴Department of Forest Production, Faculty of Forestry,
Universiti Putra Malaysia, 43400 UPM Serdang, Selangor, Malaysia

⁵Centre for Languages and Human Development, Universiti Teknikal Malaysia Melaka (UteM),
Hang Tuah Jaya, 76100, Durian Tunggal, Melaka, Malaysia

Abstract: Front-wheel direct-driven dual motors of an electric vehicle (EV) with a single controller configuration offer great potential and flexibility for improving system performance, efficiency and safety. The objective of the paper is to design a new load torque estimator of Direct Torque Control (DTC) by merging the electrical model with the mechanical model of an EV traction system to improve the dual motors single controller configuration. The electrical model utilise Space Vector PWM (SVPWM) DTC control of dual induction motors fed Five-leg Inverter (FLI) while the mechanical model takes the 14DOF vehicle dynamic model as its main structure. The new technique used is by integrating lateral force with longitudinal force produced at the touch point of a tyre with road surface as the input to the new load torque estimator of DTC. The new load torque estimator technique results were, then, compared with the standard load torque estimator that used the voltage and current feedback only. The findings showed that while torque estimator of conventional DTC had no effect of steering angle on the speed, torque and current performance of the motors, the new load torque estimator showed a significant impact. The speed, torque and current responds of the motors now have precisely been estimated; following the trajectory of the steering angle. Hence, for future research the new load torque estimator with the accurate and precise speed and torque response can further be utilized in stability, slip and skid and traction control or even for electronic braking system.

Key words: Traction control % Direct Torque Control (DTC) % Multi-machine single converter % Load torque estimator % EV modelling % Electric differential

INTRODUCTION

Presently, two wheels traction motor drives have gained increasing interest in the studies of electric

vehicle (EV) control system. The purpose is to find a solution of dependencies on one single traction motor. The drawback of using only a single motor to drive an EV with a weight of around 3000 kilogramme is that it

Corresponding Author: Nurazlin Mohd Yaakop, Faculty of Electrical Engineering, Universiti Teknikal Malaysia Melaka (UTeM), Hang Tuah Jaya, 76100, Durian Tunggal, Melaka, Malaysia.
Tel: +60195744088, E-mail: nurazlin@msi.unikl.edu.my.

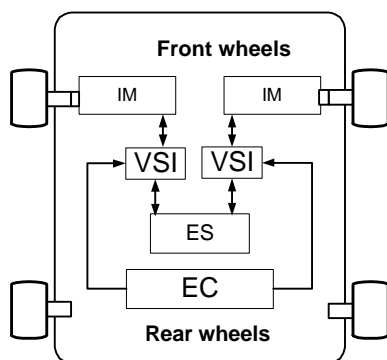


Fig. 1: Dual inverters to supply dual motors EV traction drive configuration (IM: Induction Motor, VSI: Voltage Source Inverter, ES: Energy Storage, ECU: Electronic Controller Unit).

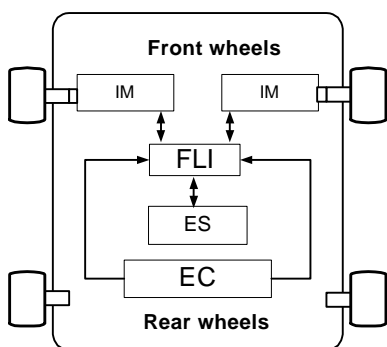


Fig. 2: Proposed EV traction drive with five-leg inverter fed two separate IM configurations (FLI: Five-leg Inverter as power converter).

needs a special design motor with a high current and low voltage which cannot be found at common industrial shops. This study uses the dual standard utility supply induction motors. Previous research on dual motors applications on current distribution control of dual directly driven wheel motors have been conducted [1]. While Tabbache *et al.* [2] proposed an adaptive electric differential to the dual wheels drive for electric vehicle motion stabilization. Hartani *et al.* [1] used the behaviour model control as the vehicle stability enhancement control for electric vehicle with dual motors drive and Nasri *et al.* [4] utilized sliding mode control. Most studies focus on the multi-motor multi-converters systems (MMS) which use two normal three-phase inverters to independently control these two motors separately as shown in Figure 1. Hence, the system's stability and robustness are attained. However, the MMS presents several drawbacks such as the increase in space, cost, weight and issues related to the efficiency of the inverters.

Emadi [5] discussed and emphasized the importance of reducing the cost of manufacturing and also the dependencies of material that is unsustainable and in the uncertainty condition like permanent magnet motor of an EV which can be commercialised. The cost can be reduced by eliminating or reducing the sensors and/or the inverter. Hence, this study uses a five-leg inverter which serves the dual motors of traction wheel drive for electric vehicle. The dual inverters have been replaced with a single inverter system as illustrated in Figure 2. In addition, the unit of power supply can also be reduced. Therefore, the complexity of communicating and transferring control signal can be reduced and thus, increased the efficiency of the working system. In industrial automation research area, multi-motors single drive systems have been introduced as one of the solutions for these MMS drawbacks. Few techniques have been proposed and some have been experimentally proven. For example, wind and unwind dual motors centre-driven using a five-leg inverter [6-7].

As for EV traction motor control, there are also other attempts done to reduce the number of inverters to control multi-motors by reducing the components; for example, reducing the switch count [8] from 6 to 4, but the motor used only two-phase power supply, the third leg was connected to both motor by capacitors. Jain *et al.* [9] introduced the idea of having FLI to control the dual motors in EV but to date, no findings was reported. Yaakop *et al.* [10] introduced electric differential (ED) in FLI traction drive system to independently control the stability of EV, but without merging it with the vehicle model. The system was tested by varying the speed command to evaluate the motor control model and ED. Driveline with dual motors requires independent control and an ED to avoid skidding and ensure stability both during the straight and cornering regime. By using ED, the usage of gear and mechanical differential could be avoided [2]. The ED system together with FLI will improve the reliability and efficiency of the overall proposed traction system.

Many studies on EV and EV motor control have examined the state-of-the-art in the scope of stability, slip control, traction control, electronic braking and even electronic stability programmes but none of them really shows how to integrate the two models namely the motor controlled part and the vehicle dynamic model part clearly for the simulations to be performed. The arising issue is how to connect the two models accurately. The previous research does not show clearly the correlation of the steering angle, longitudinal and

lateral forces with the motor drive control algorithm. An effective and accurate simulation platform for simulating the electric motor control especially for the dual motors traction wheel drive of an EV application is strongly needed. Thus, the success of this integrate model and simulation can be applied to electronic stability programmes and electronic braking system for EV. Furthermore, the modelling technique used to model motor controller, dynamic vehicle and magic tyre model have been tested and validated [12-16]. This study proposed a new technique by integrating lateral force with longitudinal force produced at the touch point of a tyre with road surface as the input to the new load torque estimator of DTC.

MATERIALS AND METHODS

Electric Differential: According to Magallan *et al.* [11] speed or torque is the main performance criterion that shows the stability condition of an EV during the straight path and cornering. The two different wheels during the straight path regime should maintain the synchronous speed and have different speed reference during cornering regime. Magallan *et al.* [11] creates the easiest way of an ED which is known as “equal torque strategy” whereby the principle of this method is to emulate the behaviour of a mechanical differential. Thus, it will always apply the same torque to both driven wheels for all vehicle manoeuvres.

For the straight-path regime, the motor rotation speeds are:

$$w_1 = w_r = \frac{v}{r} \quad (1)$$

For the second regime, cornering regime is shown in Figure 3. The rotation speed for each motor is different. For example, in the right turning way, the speeds are expressed as

$$\left\{ \begin{aligned} w_1 &= \frac{2v}{\left(1 + \frac{2d}{r}\right)} = \frac{v}{r} + \Delta w \\ w_r &= \frac{2v}{\left(1 + \frac{2d}{r}\right)} = \frac{v}{r} - \Delta w \\ \Delta w &= d \frac{v}{r^2} \end{aligned} \right. \quad (2)$$

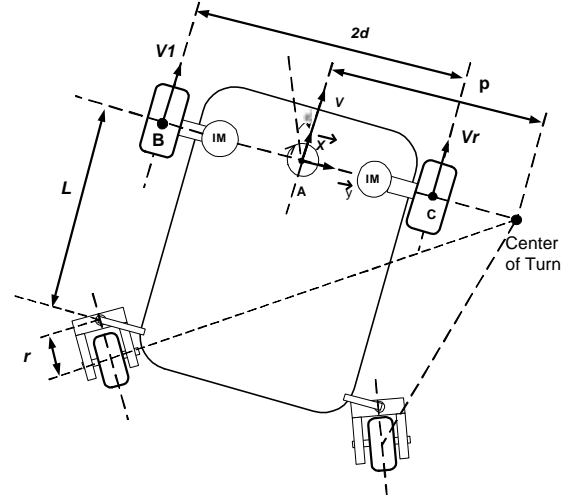


Fig. 3: Electric vehicle driving trajectory model

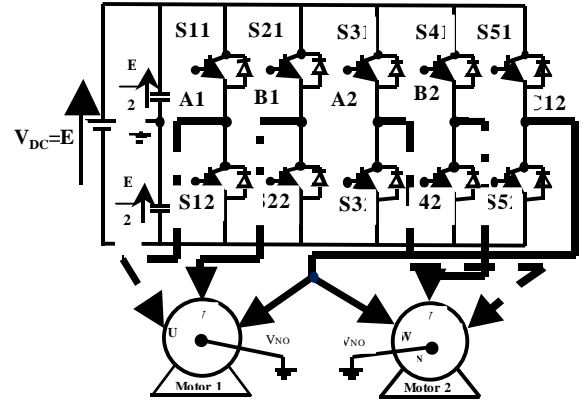


Fig. 4: Main circuit topology of two three-phase IM fed by FLI

Where ΔT is the speed difference between the inner wheel and outer wheel. For example, while performing a right turn, the right wheel is the inner wheel while the left wheel is the outer wheel [19].

A Five-Leg Inverter Topology: A five-leg two-motor drive structure offers a saving of two switches when compared with the standard dual three phase VSI. Thus, it offers a reduction in the inverter structure complexity and also it enables the control of two three-phase AC motors with only one DSP. This advantage can be utilized in the dual traction motors of an EV and there is a possibility of reducing the drivelines structure complexity and devices. Figure 4 shows the main structure of the FLI.

Both motors need three inputs. While the C leg works as a common leg, leg A1 and B1 are connected to phase U and V of motor 1 (M1). Leg A2 and B2 are

connected to phase U and phase V of motor 2 (M2), respectively. Switching functions, S_i ($i=1, 2, 3, 4, 5$), are defined as $S_i = 1$ when the upper switch is on and $S_i = 0$ when it is off. A total of 32 switching states (2^5) in a five-leg VSI is available for controlling the two motors [2]. The maximum voltage value at terminal of an open switch is always equalled to the DC voltage V_{DC} (i.e. at rated operating range of one motor can be achieved). This voltage must be greater than the greatest phase-to-phase voltage. Thus, the capability of FLI leads to a reduction of the supply voltages for the IMs. As the results, speed range and load disturbances in which the motors can handle are also reduced.

Direct Torque Control and Induction Motor Model:

The behaviour of IM in DTC drives principal can be described in terms of space vectors by the following equations, written in the stator stationary reference frame [17-18]:

$$\mathbf{n}_s = r_s \mathbf{i}_s + \frac{d\mathbf{j}_s}{dt} \quad (3)$$

$$0 = r_r \mathbf{i}_r - j\omega_r \mathbf{j}_r + \frac{d\mathbf{j}_r}{dt} \quad (4)$$

$$\mathbf{j}_s = L_s \mathbf{i}_s + L_m \mathbf{i}_r \quad (5)$$

$$\mathbf{j}_r = L_r \mathbf{i}_r + L_m \mathbf{i}_s \quad (6)$$

$$T_e = \frac{3}{2} P |\mathbf{j}_s| |\mathbf{i}_s| \sin d \quad (7)$$

Where P is the number of pole pairs, T_r is the rotor electric angular speed in rad/s, L_s , L_r and L_m are the motor inductances, r_s is the stator resistance, [ohm] S and $*$ is the angle between the stator flux linkage and the stator current space vectors. Based on (1) the d^s - and q^s - axis stator flux in the stationary reference frame can be written as:

$$\mathbf{j}_{s,d} = \int (v_{s,q} - i_{s,d} r_s) dt \quad (8)$$

$$\mathbf{j}_{s,q} = \int (v_{s,d} - i_{s,q} r_s) dt \quad (9)$$

In terms of switching states S_a , S_b and S_c (which can either be 0 or 1) the voltage vectors in (7) are given by:

$$v_{s,d} = \frac{1}{3} V_{dc} (2S_a - S_b - S_c) \quad (10)$$

$$v_{s,q} = \frac{1}{\sqrt{3}} V_{dc} (2S_b - S_c) \quad (11)$$

Table 1: Induction Motor parameters (for both motors)

Parameter	Unit
Stator resistance, R_s	7.83S
Rotor resistance, R_r	7.55S
Stator self inductance, L_s	0.4751H
Rotor self inductance, L_r	0.4751H
Mutual inductance, L_m	0.4535H
Number of poles, p	4
Stator flux rated	0.954 Wb
Torque rated	13 Nm
Power	1.5 kW
Speed	1460rpm

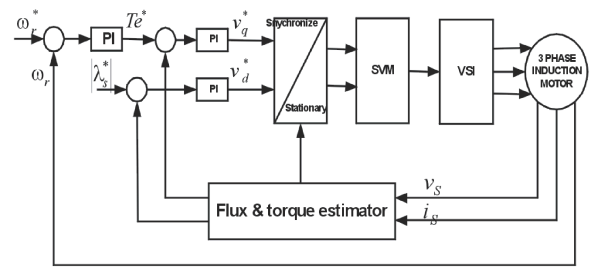


Fig. 5: Block diagram of normal DTCSVPWM three-phase IM drive

The electromagnetic torque given in (6) can be written in the $d^s - q^s$ coordinates as:

$$T_e = \frac{3}{2} P (\mathbf{j}_{s,d} i_{s,d} - \mathbf{j}_{s,q} i_{s,q}) \quad (12)$$

The two similar types of three phases IM are used in the simulation studies and details about the motor parameters are shown in Table 1 below:

DTC has a simple structure and fast torque response advantages as depicted in Figure 5. The basic principle of DTCSVPWM algorithm and also a five-leg inverter can be found [14].

Vehicle dynamic model: The dynamics of a 14-DOF vehicle model are derived and integrated with an analytical equation of tyre dynamics model, namely magic tyre model by Pacejka [11]. The dynamic car modelling is divided into two parts: ride model or also known as vertical dynamic model and handling model with a 7-DOF each

Ride Model: Ride model is basically the 7-DOF vertical influence experienced by the passengers in a car when the car moves on the road surface and is not derived from the driving act. Such translational motions like the vertical displacement up and down because of bumper, roll to the left side and right side during cornering, pitch effect during braking and accelerating and

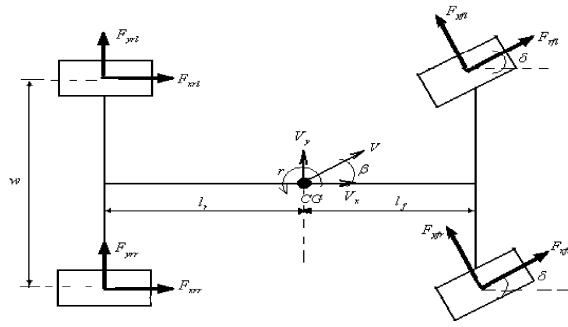


Fig. 6: Handling model of vehicle dynamic model [11]

unsprung-mass vertical displacement by the four wheels are included in this developed model. Ride model consists of a car body (single sprung mass) connected to the four wheels (unsprung masses) that are front-left, front-right, rear-left and rear-right wheels at each side turn. The suspensions between the sprung mass and unsprung masses are modelled as passive viscous dampers and spring elements. While, the tyres are modelled as simple linear springs without damping. For simplicity, all pitch and roll angles are assumed to be small [3]. The force balance on sprung mass is given as

$$M_s \ddot{\delta}_s = F_{fl} + F_{fr} + F_{rl} + F_{rr} \quad (13)$$

Where M_s is the vehicle sprung mass, F_{ij} is the body vertical acceleration, F_{ij} is defined as suspension force namely spring and damper force at each corner of the vehicle with the index (i) indicating front, (f) or rear (r) tyres and (j) indicating left (l) or right (r) tyres.

Handling Model: The other 7-DOF is in the handling model. Figure 6 shows the free body diagram of a handling model. This model consists of seven motions or moments that is triggered by the driving act; longitudinal acceleration, lateral acceleration, yaw acceleration or vertical body displacement and the other four comes from each wheel reaction. Each of this DOF can be presented into equations to perform as a handling model in vehicle dynamic model.

Acceleration in longitudinal x -axis is defined as

$$\mathbf{n}_x = a_x + v_y \dot{\gamma} \quad (14)$$

By summing all the forces in x -axis, longitudinal acceleration can be defined as

$$a_x = \frac{F_{xfl} \cos \delta + F_{yfl} \sin \delta + F_{xfr} \cos \delta + F_{yfr} \sin \delta + F_{xrl} + F_{xrr}}{m_t} \quad (15)$$

Similarly, acceleration in lateral y -axis is defined as

$$\dot{v}_y = a_y - v_x \dot{\gamma} \quad (16)$$

By summing all the forces in lateral direction, lateral acceleration can be defined as

$$a_y = \frac{F_{yfl} \cos \delta - F_{xfl} \sin \delta + F_{yfr} \cos \delta - F_{xfr} \sin \delta + F_{yrl} + F_{yrr}}{m_t} \quad (17)$$

where;

F_{xij} and F_{yij} denote the tyre forces in the longitudinal and lateral directions, respectively, with the index (i) indicating front (f) or rear (r) tyres and index (j) indicating left (l) or right (r) tyres. The steering angle is denoted by δ , the yaw rate by $\dot{\gamma}$ and m_t denotes the total vehicle mass. The longitudinal and lateral vehicle velocities v_x and v_y can be obtained by the integration of \dot{v}_y and \dot{v}_x [11]. The behaviour of the vehicle model is then verified using a vehicle dynamics software namely CarSimEd. Model verification using CarSimEd software is performed in both subsystem and a complete system levels before being validated using a real vehicle [11].

The equations can be expressed as follows [19]

$$m(\dot{v}_x \quad v_y \quad \mathbf{g}) = X_1 + X_2 + X_3 + X_4 \quad (18)$$

$$m(\dot{v}_y \quad v_x \quad \mathbf{g}) = Y_1 + Y_2 + Y_3 + Y_4 \quad (19)$$

$$J_z \dot{\gamma} = I_f(Y_1 + Y_2) - I_r(Y_3 + Y_4) - \frac{d_f}{2}(X_1 + X_2) + \frac{d_r}{2}(X_3 + X_4) \quad (20)$$

Two different tests are done in the simulation that is the straight path regime and cornering test which employ the double lane change standard test. The double lane change test procedure consists of driving a vehicle through a set track which simulates a lane change manoeuvre. The purpose of this test procedure is to subjectively determine the road holding ability and handling characteristics of a vehicle [20].

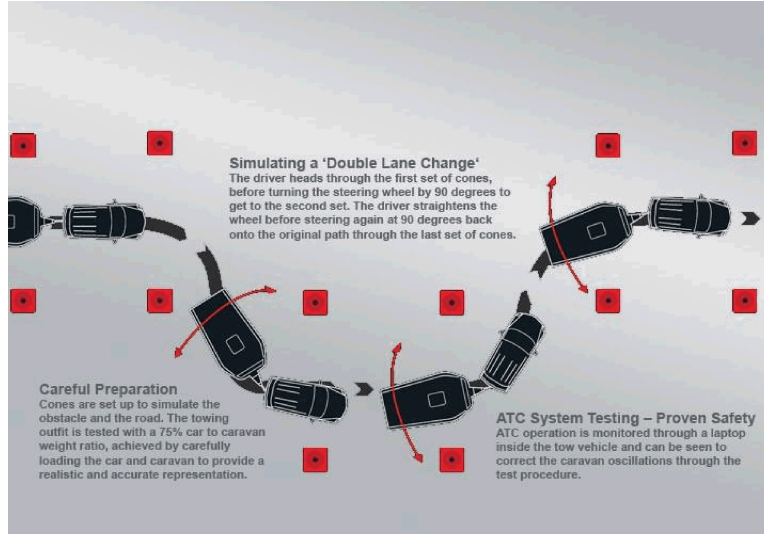


Fig. 7: Double lane change manoeuvre illustration [21]

The Proposed Merging Model: In order to obtain the accurate actual speed and estimated speed based on the reference speed, this study proposed a new torque load estimator based on vehicle handling models. The wheel equation of motion is stated as

$$F_{xf} R_w - T_{bf} + T_{af} = I_w \dot{\omega}_f \quad (21)$$

$$F_{xr} R_w - T_{br} + T_{ar} = I_w \dot{\omega}_r \quad (22)$$

Where T_f and T_r are the angular velocity of the front and rear wheels, I_T is the inertia of the wheel about the z- axle, R_T is the radius of the wheel, T_{bf} and T_{br} are the applied braking torques and T_{af} and T_{ar} are the front and rear wheels applied throttling torques. From the vehicle dynamic models, the lateral, X and longitudinal, Y forces for each tyre can be calculated separately.

where

$$\begin{aligned} X_i &= Fx_i \cos d_i + Fy_i \sin d_i \quad i=1,2,3,4 \\ Y_i &= Fx_i \sin d_i + Fy_i \cos d_i \end{aligned} \quad (23)$$

Each point of tyre has different total of forces acting. The tyres can be in one direction and each will have x-axis and y-axis forces exist at the tyre plane. These planar axis forces can then be transformed to longitudinal and lateral forces (the x-axis and y-axis forces of the EV body direction). Different forces summation can be accumulated depending on the direction. If the steering angle ($*$) is equalled to zero, only longitudinal forces exist. If the steering angle input is

positive, the EV will be assumed to be on the right turn. The total sum of forces exists at each tyre for right corner would be

where;

Total forces = Longitudinal forces + Lateral forces
(following direction of the wheels)

$$\text{forces, right corner} = Fx_i \cos * + Fy_i \sin * - Fx_i \sin * + Fy_i \cos * \quad (24)$$

while with negative steering angle input, the EV is doing left turn. The total sum of forces exists at each tyre for left corner would be

$$\text{Total forces, left corner} = Fx_i \cos * + Fy_i \sin * - Fx_i \sin * - Fy_i \cos * \quad (25)$$

The mechanical motor equation to calculate the torque would be

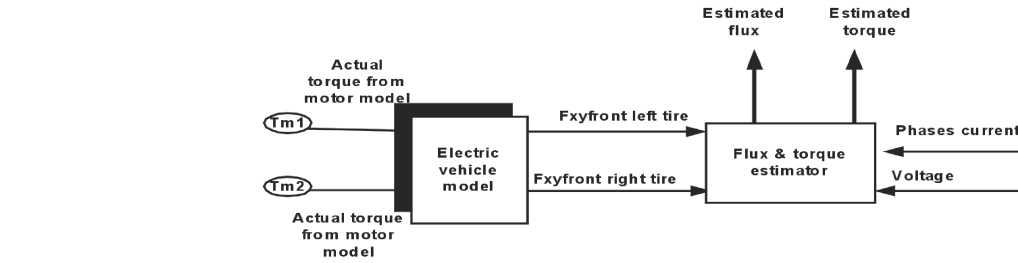
$$T_{motor} = J \frac{d\omega}{dt} + T_{friction} + T_{load} \quad (26)$$

$$T_{motor} = T_{wheel} \quad (27)$$

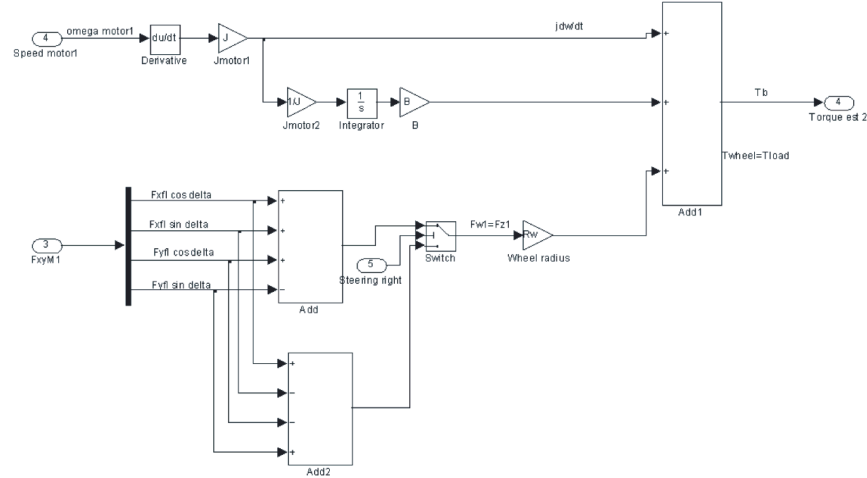
$$T_{load} = T_{loadwheel} = RFw \quad (28)$$

Where;

$$Rfwi = (Fx_i + Fy_i) \quad (29)$$



(a) Block diagram



(b) MATLAB/Simulink subsystem

Fig. 8: Block diagram and subsystem of the proposed torque load estimator

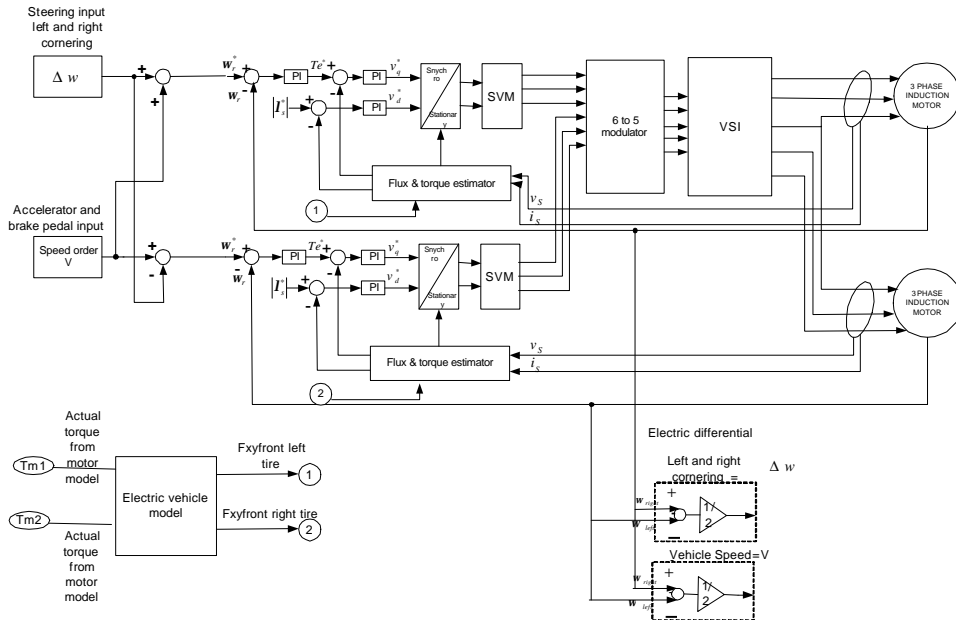
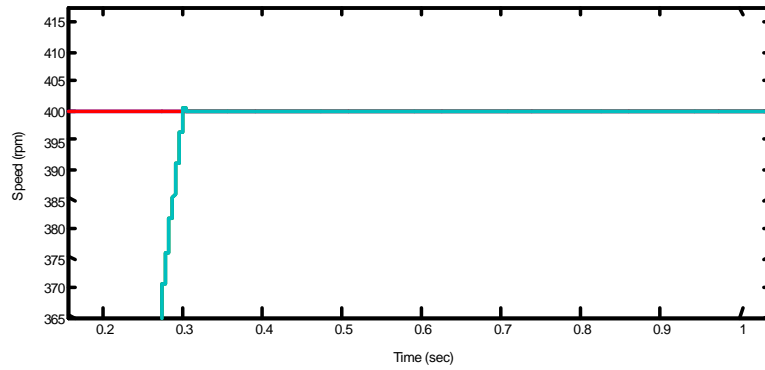


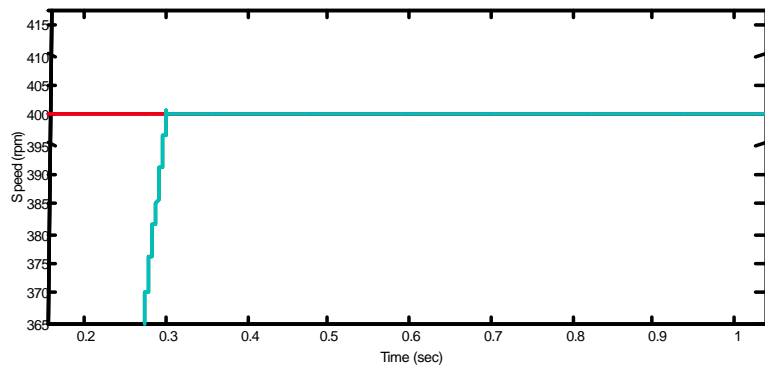
Fig. 9: The overall modelling and simulation of the proposed system.

From the equations above, the load torque of the wheel can be estimated by using the forces obtained from the vehicle model. Then, the motor torque can be estimated as well. Figure 8 shows

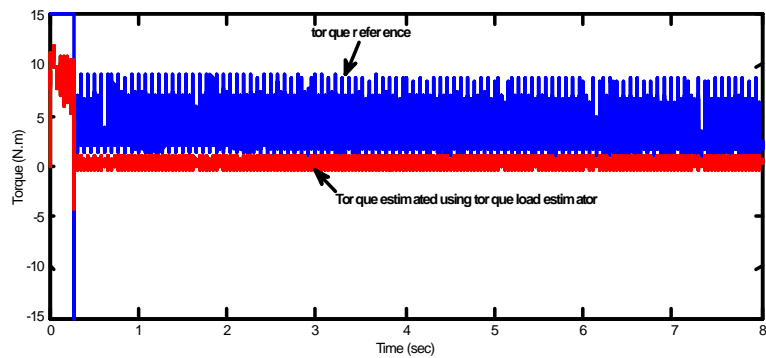
the block diagram of the proposed new load torque estimator to replace the normal DTC torque estimator. The overall simulation diagram can be found in Figure 9.



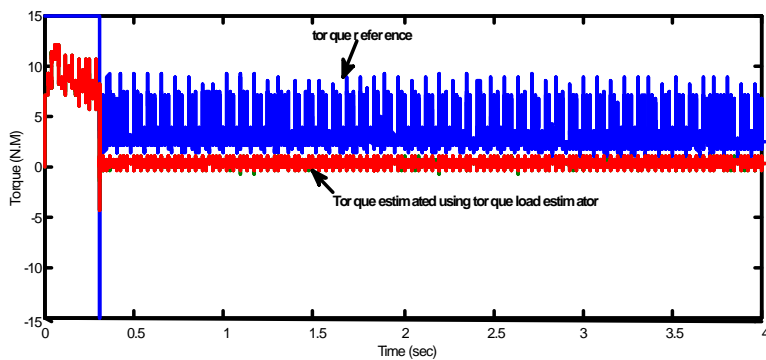
(a) Enlarge speed response with normal DTC torque estimator



(b) Enlarge speed response with proposed torque load estimator



(c) Torque response with normal DTC torque estimator (both motors give the same responds)



(d) Torque response with proposed torque load estimator (both motors give the same responds)

Fig.10: Straight path lane test

RESULTS AND DISCUSSION

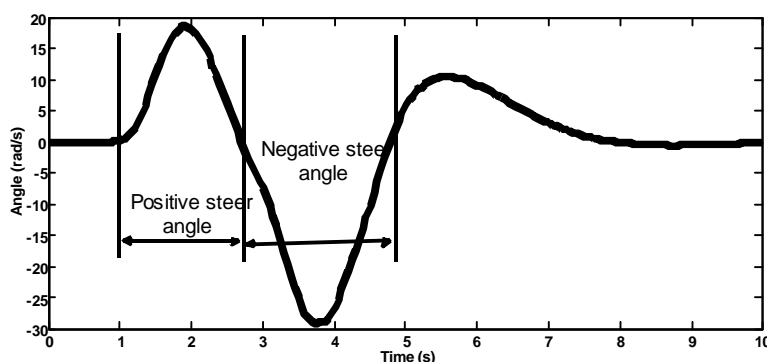
The simulations of the proposed new load torque DTC estimator with ED for FLI using SVPWM merging duty cycle technique were conducted using MATLAB/Simulink. The two IM rated parameters are given in Table 1. Two speed profiles with three different steering angle input performance was evaluated namely the straight path regime in which the two motors have synchronous speed and the cornering regime. The steering angle input data from the vehicle model was provided. The cornering regime test used the standard double lane change test. The outer wheel moved faster than the inner wheel if the EV needed to perform a cornering regime. The motor torque also varied accordingly with the effect of the lateral and longitudinal forces. These results can be compared to other works [2, 16, 22].

The result of the first test, known as straight path, can be found in Figure 8(a-d). It shows the speed and torque response for both torque estimators: the normal DTC that used phase current and voltage and the one used the new proposed torque load estimator. The results showed that there

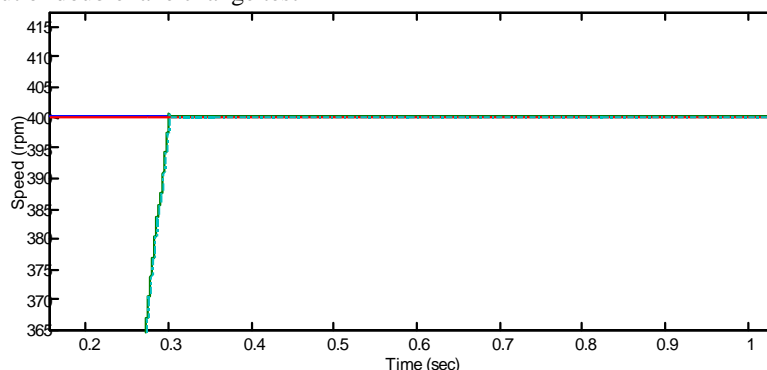
is not much difference in terms of speed response since the torque of the two motors traction wheel drive did not change.

The next manoeuvre for verification process of the vehicle model is the double lane change manoeuvre with the speed of 400 rpm. Double lane change is one of the handling manoeuvres that are used to evaluate the road holding of the vehicle. Figures 10 and 11 show the responses of model and vehicle behaviours obtained from the simulations.

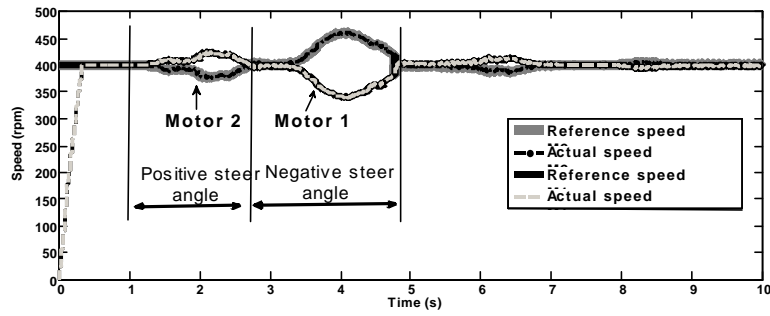
It can be depicted from Figure 11(b), that there is no effect to the normal DTC system even though the steering angle (Figure 11(a)) is changing. Figure 11(c) shows the speed response while 11(d) illustrates the estimated torque response. The three phase current response of the motor 1 as samples are depicted in Figure 11(e-g). The new proposed torque load estimator can estimate the speed following the steering input and controlling the dual motors. The speed of the inner wheels and outer wheels is changing which depends on the steering angle input. The torque response also follows accordingly. The torque estimated by proposed load torque estimator is much more accurate, thus producing a more precise, correct and fast speed response in controlling the motors.



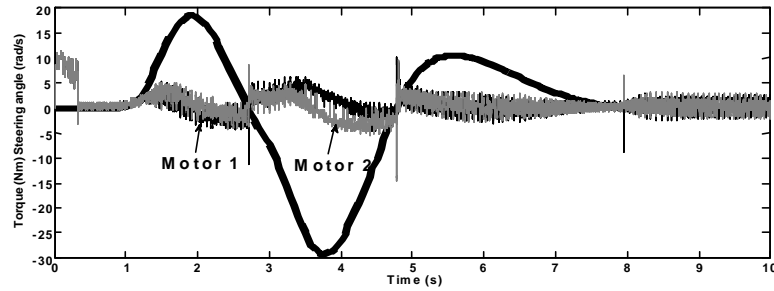
(a)Steering angle input of double lane change test



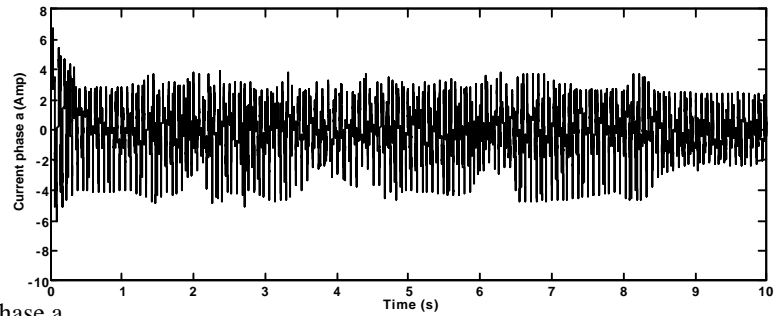
(b)Speed response with normal DTC torque estimator



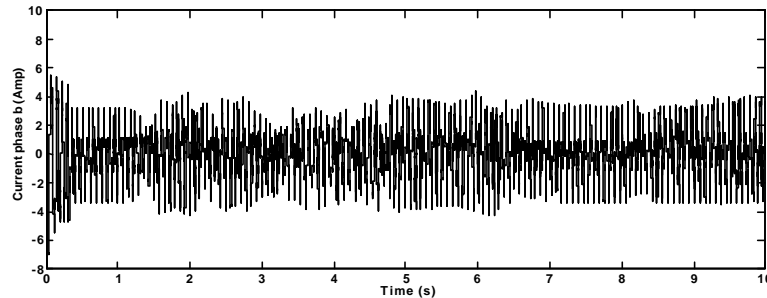
(c) Speed response with proposed torque load estimator



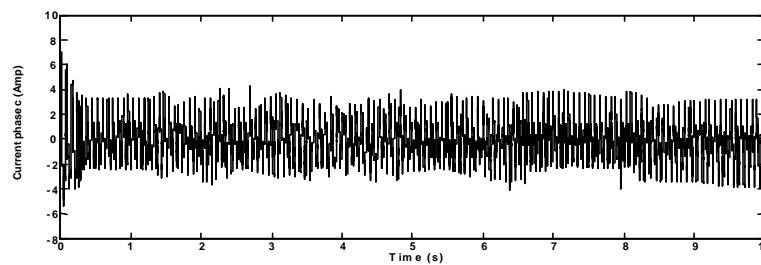
(d) Torque response of the proposed load torque estimator compared with steering angle input



(e) current response phase a



(f) current response phase b



(g) current response phase c

Fig. 11: Second test the double lane change manoeuvre

CONCLUSION

This paper has presented a new load torque estimator of direct torque control (DTC) that relate the electrical model with vehicle dynamic model accurately by integrating the steering angle input, longitudinal force and lateral force into its new design controller based on FLI. It is expected that when having a cornering regime, the inner wheel and outer wheel should give different speed response. Based on the result of this study, there was no effect of steering angle input on the torque estimated by conventional DTC (using current and voltage). The conventional system if given a different speed profile can be controlled to follow the speed, but if given a different steering angle, it could not be detected on its own. This is different compared to the new load torque estimator which it can accurately estimate the speed, torque and current responses correlated with the trajectory of the steering angle. The important of this study is it can improve the stability control of dual motor EV traction drive system by inculcate the effect of the longitudinal and lateral forces at each touching point of the tyre in electric motor control system. These results validate the new proposed load torque estimator successfully for front-wheel direct-driven dual motors (EV) with a FLI controller. Hence, for future research the new load torque estimator with the accurate and precise speed and torque response can further be utilized in stability, slip and skid and traction control or even for electronic braking system.

REFERENCES

1. Yang, Y.P. and C.P. Lo, 2008. Current distribution control of dual directly driven wheel motors for electric vehicles. *Journal of Control Engineering Practice*, 16(11): 1285-1292.
2. Tabbache, B., A. Kheloui and M.E.H. Benbouzid, 2011. An adaptive electric differential for electric vehicles motion stabilization. *IEEE Transactions on Vehicular Technology*, 60(1): 104-110.
3. Hartani, K., Y. Miloud and A. Miloudi, 2011. Vehicle Stability Enhancement Control for Electric Vehicle. *Electric Vehicle - Modelling and Simulations. InTechOpen Book*. ISBN 978-953-307-477-1.
4. Nasri, A., A. Hazzab, I.K. Bousserhane, S. Hadjeri and P. Sicard, 2009. Fuzzy-Sliding Mode Speed Control for Two Wheels Electric Vehicle Drive. *Korean Journal of Electrical Engineering and Technology*, 4(4): 499-509.
5. Emadi, A., Y.J. Lee and K. Rajashekara, 2008. Power electronics and motor drives in electric, hybrid electric and plug-in hybrid electric vehicles. *IEEE Transactions on Industrial Electronics*, 50(6): 2237-2245.
6. Jones, M., S.N. Vukosavic, D. Dujic, E. Levi and P. Wright, 2008. Five-leg inverter PWM technique for reduced switch count two-motor constant power applications. *Electric Power Applications IET*, 2(5): 275-287.
7. Dujic, D., M. Jones, E. Levi and S.N. Vukosavic, 2008. A two-motor centre-driven winder drive with a reduced switch count. *34th Annual Conference of IEEE Industrial Electronics (IECON)*, Florida Hotel and Conference Center, Orlando, Florida, USA, pp: 1106-1111.
8. Ledezma, E., B. McGrath, A. Muñoz and T.A. Lipo, 2001. Dual AC-drive system with a reduced switch count. *IEEE Transactions on Industry Applications*, 37(5): 1325-1333.
9. Jain, M. and S. Williamson, 2010. Modeling and analysis of a 5-leg inverter for an electric vehicle in-wheel motor drive. *23rd Canadian Conference on Electrical and Computer Engineering (CCECE)*, Telus Convention Center, Calgary, Alberta, Canada, pp: 1-5.
10. Yaakop, N.M., Z. Ibrahim, M. Sulaiman and M.H.N. Talib, 2012. Speed performance of SVPWM direct torque control for five leg inverter served dual three-phase induction motor. *IEEE International Conference on Power Engineering and Optimization (PEOCO)*, Melaka, Malaysia, pp: 323-328.
11. Ahmad, F., K. Hudha, F. Imaduddin and H.J. amaluddin, 2010. Modelling, validation and adaptive PID control with pitch moment rejection of active suspension system for reducing unwanted vehicle motion in longitudinal direction. *International Journal of Vehicle Systems Modelling and Testing*, 5(4): 312-346.
12. Ahmad, F., K. Hudha and H.J. amaluddin, 2009. Gain scheduling PID control with pitch moment rejection for reducing vehicle dive and squat. *International Journal of Vehicle Safety*, 4(1): 45-83.
13. Ahmad, F., Z.A. Kadir and H. Jamaluddin, 0000. Pid Controller with Roll Moment Rejection for Pneumatically Actuated Active Roll Control (Arc) Suspension System. In *Tech Open*.

14. Yaakop, N.M., Z. Ibrahim, M. Sulaiman, J.M. Lazi, A.S.A. Hasim and F.A. Patakor, 2012. Electric differential with SVPWM direct torque control using five-leg inverter for electric vehicles. *Journal of Theoretical and Applied Information Technology (JATIT)*, 46(2): 599-609.
15. Talib, M.H.N., Z. Ibrahim, N.A. Rahim and N.M. Yaakop, Development of combined vector and Direct Torque Control methods for independent two induction motor drives. *IEEE International Conference on Power Engineering and Optimization (PEOCO)*, Melaka, Malaysia, pp: 78-83.
16. Magallan, G.A., C.H. De Angelo and G.O. Garcia, 2011. Maximization of the Traction Forces in a 2WD Electric Vehicle. *IEEE Transactions on Vehicular Technology*, 60(2): 369-380.
17. Jidin, A., N.R.N. Idris, A.H.M. Yatim, T. Sutikno and M.E. Elbuluk, 2011. Extending switching frequency for torque ripple reduction utilizing a constant frequency torque controller in DTC of induction motors. *Journal of Power Electronics*, 11(2): 148-155.
18. Sedaghati, A., 2006. A PI controller based on gain-scheduling for synchronous generator. *Turk Journal Electrical Engineering*, 14(1): 1300-0632.
19. Zhao, Y. and J. Zhang, 2009. Modelling and simulation of the electronic differential system for an electric vehicle with two-motor-wheel drive. *International Journal of Vehicle Systems Modelling and Testing*, 4(1): 117-131.
20. Mattes, S., 2003. The lane change task as a tool for driver distraction evaluation. *IHRA-ITS Workshop on Driving Simulator Scenarios*, Dearborn, Michigan (www-nrd.nhtsa.dot.gov/IHRA/ITS/MATTES.pdf).
21. What is the ELK Test? AL-KO. Retrieved 2013, from: <http://www.al-ko.co.uk/pages/what-is-the-elk-test--3.html>.
22. Magallan, G.A., C.H. De Angelo and G.O. Garcia, 2009. A neighbourhood-electric vehicle development with individual traction on rear wheels. *International Journal of Electric and Hybrid Vehicles*, 2(2): 115-136.